

RESEARCH

Open Access



Early embryonic development of the German cockroach *Blattella germanica*

Ariel Bar-Lev Viterbo¹ , Judith R. Wexler¹ , Orel Mayost Lev-Ari¹ and Ariel D. Chipman^{1*}

Abstract

Background Early embryogenesis is characterized by dramatic cell proliferation and movement. In most insects, early embryogenesis includes a phase called the uniform blastoderm, during which cells evenly cover the entirety of the egg. However, the embryo of the German cockroach, *Blattella germanica*, like those of many insects within the super order Polyneoptera, does not have a uniform blastoderm; instead, its first cells condense rapidly at the site of a future germband. We investigated early development in this species in order to understand how early gene expression is or is not conserved in these insect embryos with distinct early cell behaviors.

Results We present a detailed time series of nuclear division and distribution from fertilization through germband formation and report patterns of expression for the early patterning genes *hunchback*, *caudal*, and *twist* in order to understand early polarization and mesoderm formation. We show a detailed time course of the spatial expression of two genes involved in the segmentation cascade, *hedgehog* and *even-skipped*, and demonstrate two distinct dynamics of the segmentation process.

Conclusions Despite dramatic differences in cell distribution between the blastoderms of many Polyneopteran insects and those of more well-studied developmental models, expression patterns of early patterning genes are mostly similar. Genes associated with axis determination in other insects are activated relatively late and are probably not maternally deposited. The two phases of segmentation—simultaneous and sequential—might indicate a broadly conserved mode of morphological differentiation. The developmental time course we present here should be of value for further investigation into the causes of this distinct blastoderm type.

Introduction

The German cockroach (*Blattella germanica*) has long been a model for post-embryonic development, and its biology has been extensively studied because of its role as a human pest [1]. Nonetheless, there only exists a brief modern description of its embryonic development [2] since Akira Tanaka presented a detailed time series of the animal's development using light microscopy and cellular dyes in the 1970s [3]. Recent work on the embryonic

development of *B. germanica* [2, 4] underscores the need to describe the early stages of embryogenesis in this species.

B. germanica is a hemimetabolous insect, a member of the superorder Dictyoptera. It has a cosmopolitan distribution and is gregarious. The species is oviparous of type B [5]; *B. germanica* females lay eggs into egg cases (oothecae), which they then carry for the duration of embryonic development (three to four weeks, depending on temperature). The process of depositing eggs into the ootheca takes approximately half a day, leading to a gradient of ages among embryos within a single egg case.

B. germanica embryogenesis differs from more well-studied model organisms in a few key ways. First, the organism lacks a uniform blastoderm; that is, there is

*Correspondence:

Ariel D. Chipman
ariel.chipman@huji.ac.il

¹ The Department of Ecology, Evolution & Behavior, The Alexander Silberman Institute of Life Sciences, The Hebrew University of Jerusalem, Edmond J. Safra Campus, 91904 Jerusalem, Israel



© The Author(s) 2024. **Open Access** This article is licensed under a Creative Commons Attribution-NonCommercial-NoDerivatives 4.0 International License, which permits any non-commercial use, sharing, distribution and reproduction in any medium or format, as long as you give appropriate credit to the original author(s) and the source, provide a link to the Creative Commons licence, and indicate if you modified the licensed material. You do not have permission under this licence to share adapted material derived from this article or parts of it. The images or other third party material in this article are included in the article's Creative Commons licence, unless indicated otherwise in a credit line to the material. If material is not included in the article's Creative Commons licence and your intended use is not permitted by statutory regulation or exceeds the permitted use, you will need to obtain permission directly from the copyright holder. To view a copy of this licence, visit <http://creativecommons.org/licenses/by-nc-nd/4.0/>.

never a stage in embryogenesis in which nuclei or cells are distributed evenly across the surface of the egg. Instead, the nuclei that will form the germ anlage cluster together in a localized area on the egg's surface. In 1972, Anderson described blastoderms of this type as direct-differentiating, as opposed to uniform [6]. Uniform blastoderms are found in holometabolous, paleopteran, and hemipteran insect embryos (with exceptions for certain lepidopteran [6, 7] and coleopteran [8–10] embryos). Direct-differentiating blastoderms are typical of polyneopteran insect embryos (with exceptions for certain orthopterans [11–13] and plecopterans [14]). Because the preponderance of research into early insect embryogenesis is concentrated in holometabolous model species with uniform blastoderms, there is a relative lack of information about how early patterning proceeds in insects with direct-differentiating blastoderms.

Among those insects with direct-differentiated blastoderms, a subset, including *B. germanica*, have embryos that form via the fusion of two regions of high cell density on the lateral sides of the egg [15, 16]. The formation of an embryo from such lateral plates is found in many, but not all, Polyneopteran orders: Zoraptera, Orthoptera, Grylloblattodea, Phasmatodea, Embioptera, and Blattodea (reviewed in [17]).

In insects, mesoderm formation is tightly linked to specific morphogenetic developments. Mesodermal tissue forms inside of the ventral furrow, which itself is the result of embryonic tissue invaginating. This phenomenon has been extensively reviewed by Anderson [6], Eastham [18], Johannsen and Butt [19], and studied specifically in *Drosophila melanogaster* [20], *Tribolium castaneum* [21], *Gryllus bimaculatus* [22], *Tenebrio molitor* [23] and others. To our knowledge, the expression of the mesodermal marker *twist* in embryos with fault-type mesoderm formation (Polyneoptera) has been investigated only in the cricket *G. bimaculatus* and only in the context of DV patterning [24]. Thus, it is unknown how genetic and morphological cues coordinate to form mesoderm in these insects.

Another notable trait of the *B. germanica* embryo is its lack of dramatic blastokinetic movement. The embryos of many other hemimetabolous insects sink in and out of yolk, and reverse orientation with respect to the egg as they develop. These movements have been described as “reversion type” blastokinesis [25]. Most holometabolous insects and some Hemipterans have embryos that display “non-reversion type blastokinesis”, that is, they remain in the same position in the egg as they develop [26]. Within Blattodea, some taxa have blastokinetic embryos, while others do not. Although embryonic movements and the extra-embryonic membranes that coordinate such movement are beyond the scope of this paper, researchers

interested in these questions may find it useful to have a developmental road map for *B. germanica* given the organism's relatively unusual lack of blastokinesis.

B. germanica is a cosmopolitan organism that interacts with humans worldwide, impacting industry and human health [27]. Phylogenetically, it sits in an understudied part of the insect tree, providing potential insights into the evolutionary paths of insect development. Practically, recent work has made CRISPR–Cas9 a viable option for genome editing in the species [28]. For all these reasons, a detailed and modern description of the animal's embryogenesis is long overdue. The differences between *B. germanica* embryogenesis and that of other, more well-studied insects discussed above mean it is not trivial to simply map events from *B. germanica* embryogenesis onto prior frameworks.

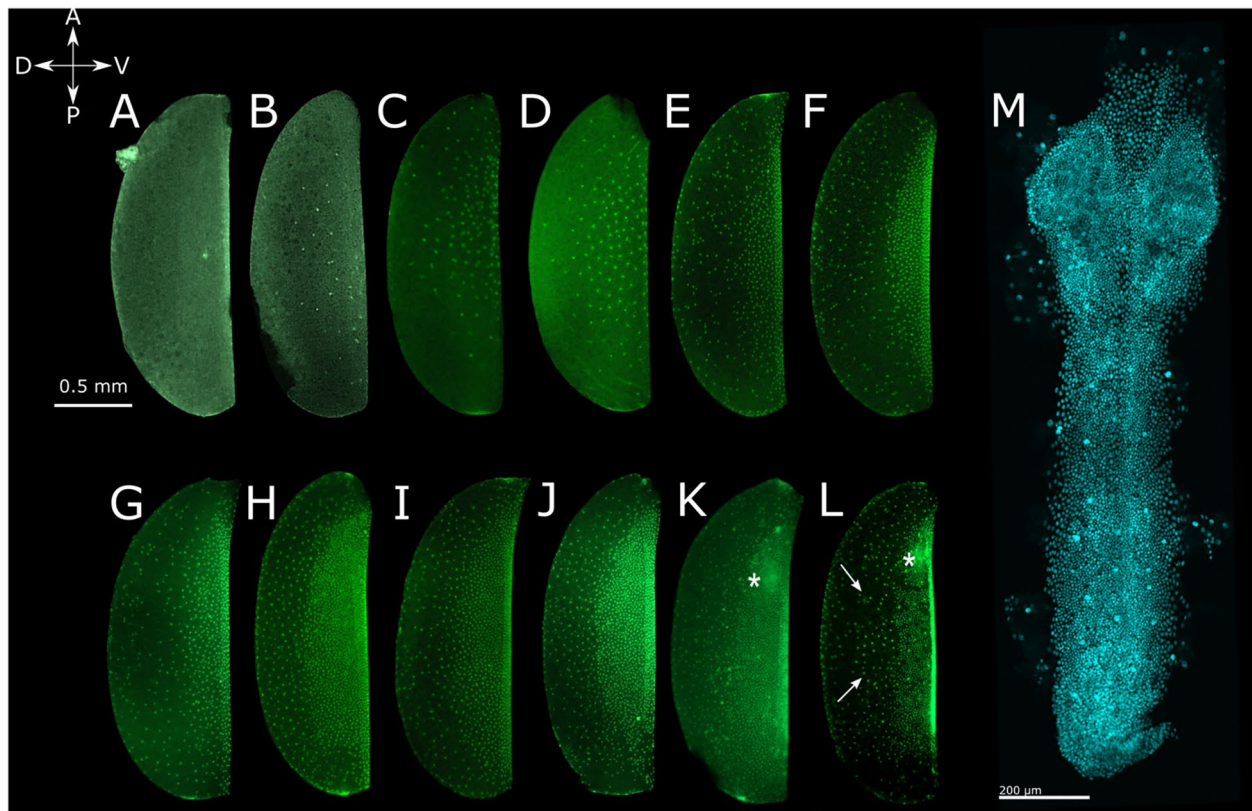
Given *B. germanica*'s phylogenetic position, studying its development can thus shed light on several other evolutionary developmental questions. Prior work from our group has highlighted the correlation between a transition in segmentation mode (simultaneous versus sequential) and final morphology (thorax versus abdomen). As we've shown in the well-studied hemimetabolous insect, *Oncopeltus fasciatus*, gnathal and thoracic segments are formed simultaneously [29], while abdominal segments arise sequentially from a segment addition zone [30]. It is unclear whether this link between tagma borders and segmentation modes is specific to *O. fasciatus* (and its relatives) or general to insects. Looking at segmentation in *B. germanica* adds an additional important phylogenetic node to answer this question.

Here, we present a time series of early *B. germanica* embryogenesis, from cleavage stages through segmentation. We show that cell division occurs in pulses in the early blastoderm stages and that cellularization happens at approximately 4–6% of development. The early patterning genes *hunchback* and *caudal* are not present in the very early embryo, suggesting they are not maternally deposited. Early stages of mesoderm formation seem similar to those reported in other insects. Segmentation appears to be of the intermediate type—that is, anterior segments are patterned almost simultaneously and posterior ones sequentially—although it is possible to observe the appearance of *hedgehog* stripes one by one.

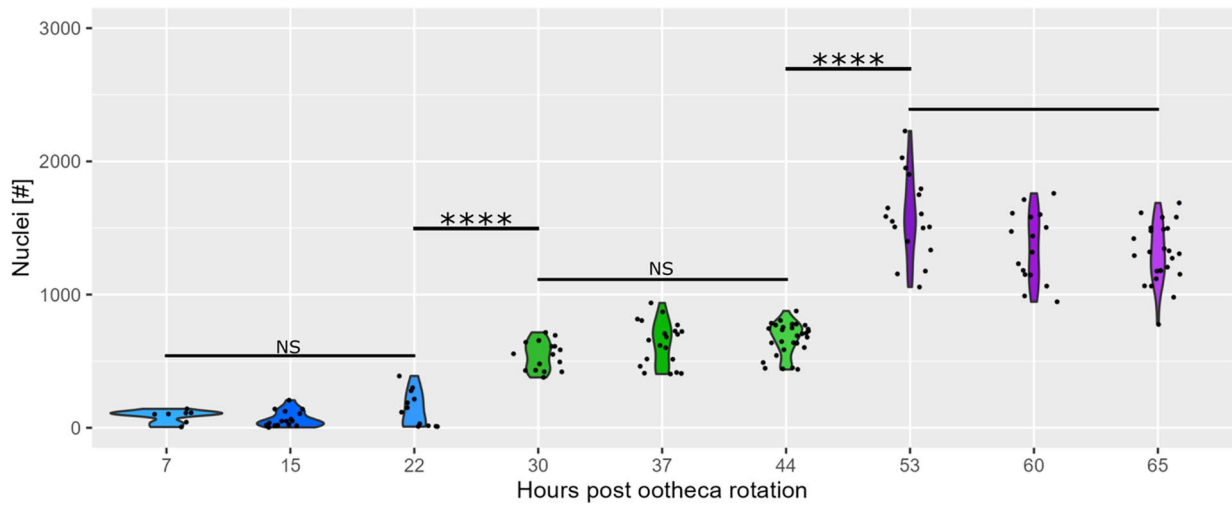
Results

Germband formation

B. germanica development takes approximately 25 days at 25°C, under our lab conditions described in the Methods. Germband formation, observed via Sytox and DAPI nuclear staining, takes about 3.5 days, or 14% of development (Fig. 1 A–M). We recorded the spatial and temporal dynamics of nuclear divisions during this time.



N Nuclei counts
Welch Anova, $p = <0.0001$



pwc: Games Howell; p.adjust: Tukey

Fig. 1 Nuclear dynamics in blastoderm and germband formation. Top panel: whole egg Sytox (A–L) and DAPI (M) staining. Embryos are arranged from youngest (A) to oldest (M). A–L Lateral view, ventral to the right, anterior top. M ventral view, anterior top, germband has been dissected out of the yolk. Asterisk in K–L marks the early head lobes, arrows mark the dorsal population of large nuclei. N Violin plot of nuclei counts taken at 7- to 8-h intervals in the 3 days after ootheca rotation. Each black dot is the count of nuclei in an individual embryo. When the time-points are divided into three bins (group A = 7,15,22 h; group B = 30,37,44; group C = 53,60,65), there are significant differences in the number of nuclei in each bin (Student’s t-test, p -value $< 2e-16$)

After counting nuclei in embryos collected every 7–8 h, we noticed two distinct pulses of cell division within the first 65 h of development (Fig. 1N). These pulses occur between hours 22–30 and 44–53. We noticed that these pulses of cell division corresponded to changes in the spatial distribution of nuclei over the surface of the egg. Combining these temporal and spatial observations, we divided early germband formation into the four following stages:

Stage 1. Days 0–1, 0–4% development (Fig. 1A–C): Cleavage and blastoderm formation stage. This stage includes cleavage and blastoderm formation. After fertilization and fusion of the male and female pronuclei near the center of the egg (Fig. 1A), energids start to proliferate and migrate to the periphery of the egg. Nuclei first appear at the ventral surface of the egg, and later they appear at the dorsal edge (Fig. 1B, C). This stage continues until the embryo has ~64–128 nuclei. At no stage do the energids show a uniform distribution over the surface of the egg—consistent with Anderson's [6] description of a direct-differential blastoderm formation in Dictyoptera. The non-uniform distribution of energids across the surface of the egg could be

explained by two phenomena: (1) non-random distribution of energid division, so that energids primarily divide on one half of the egg surface, or (2) energid migration, a scenario in which energid division occurs evenly across the surface of the egg, but the products of the division migrate to the ventral surface of the egg. Anti-phospho-histone 3 staining suggests the second explanation is correct during stage 1 and stage 2, as we observed dividing energids across the surface of the egg during these two stages (Fig. S1, n=7 embryos in stage 1 and 11 embryos in stage 2).

Stage 2. Days 1–2.5, 4–10% development (Fig. 1D–J): Syncytial blastoderm stage. At this stage, the egg can be separated into 2 regions (Fig. 1D–J). The dorsal region is populated by a low density of energids, while on the ventral half of the egg, we find bilaterally paired regions of higher energid density. We hypothesize that energids from the dorsal region are migrating to the ventral region during this stage, but because of system limitations (i.e., no live imaging nor nuclear tagging and tracking), we cannot test this hypothesis explicitly. Cellularization occurs at the middle of this stage (see below, Cellularization section) (Fig. 2).

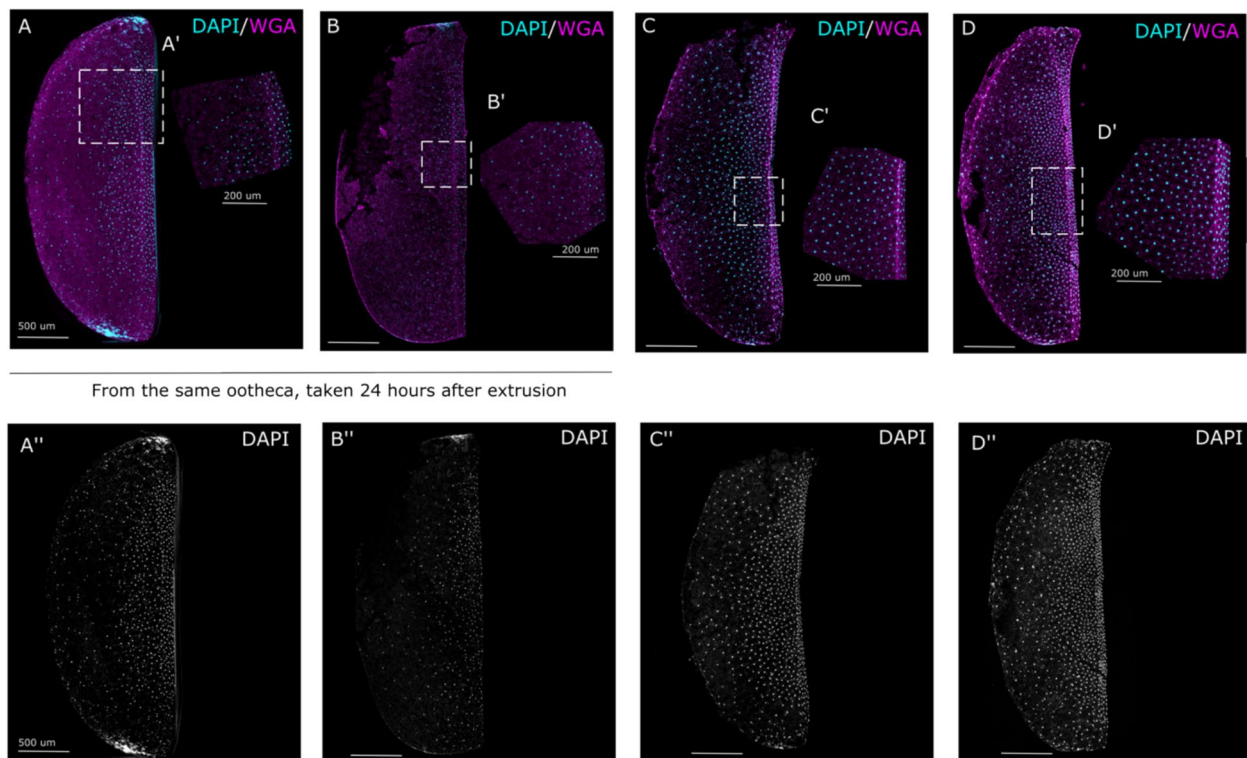


Fig. 2 Cellularization occurs around stage 2. Embryos stained with DAPI and wheat germ agglutinin (WGA). Ventral side facing right. The top row shows both DAPI (blue) and WGA (red). White boxes show areas of higher magnification in panels **A–D'**. The bottom row shows DAPI in grey from each embryo displayed in the panel directly above it. **A** Cell membranes do not appear visible with WGA in an embryo collected at 24 h (4% of developmental time) after ootheca extrusion, but cell membranes are detected in embryo **(B)** collected from the same ootheca. **C, D** Embryos collected from the same ootheca 24–48 h (4–8% developmental time) post-extrusion show visible cell membranes as detected with WGA

Stage 3. Days 2.5–3.5, 10–14% development (Fig. 1K, L): Germ anlage/rudiment stage. At this stage, two populations of nuclei can be identified in the dorsal half of the egg. One population consists of slightly larger, presumably polyploid [31–33] nuclei that are destined to become serosal cells (Fig. 1L marked with an arrow). The cells in the second population in the dorsal half of the egg are smaller and of equivalent size to the cells in the germ rudiment. We noticed a reduction in cell division on the dorsal side of the egg during stage 3 (Fig. S1, $n=5$ embryos counted). As cell division continues on the ventral side of the egg, a subset of anterior cells further condenses in the space where the head lobes will develop (Fig. 1K, L, marked with an asterisk).

Stage 4. Days 3.5 and on (Fig. 1M): Early germband stage. Following an accelerated phase of cellular condensation, the paired regions of higher cellular density fuse at the ventral region of the egg, starting at the posterior end and fusing towards the anterior, to form the bipartite germband (Fig. 1M). We define the end point of stage 4 as the complete fusion of lateral plates.

Cellularization

We used wheat germ agglutinin (WGA) to look for the presence of cell membranes in embryos from oothecae 24–48 h post-extrusion. Using an Eclipse 80i Nikon Microscope, we detected evidence of cell membranes in only one of five embryos examined from an ootheca 24 h post-extrusion (Fig. S2). We took this embryo (Fig. 2B), plus a second embryo from the same ootheca with no discernable evidence of cell membranes (Fig. 2A), to an Olympus FV1200 confocal microscope for further imaging. In the embryo with evidence of cell membrane formation from the 24 h-old ootheca, the WGA appeared to be condensing around nuclei (Fig. 2B"). Surprisingly, the embryo without visible cell membranes had more nuclei than the embryo with membranes. The WGA signal is

seen more tightly bound around nuclei in two embryos taken from an older ootheca between 24 and 40 h post-extrusion. By mid to late stage 2, embryonic nuclei are cellularized.

Segmentation

The determination of embryonic segments begins in embryonic stage 3 (Fig. 3). We used both chromogenic in situ (cISH) and Hybridization Chain Reaction (HCR) to investigate the expression of *B. germanica hedgehog* (*Bg-hh*) (Fig. 3), an arthropod-wide marker of segment formation [34] and *B. germanica even-skipped* (*Bg-eve*) (Fig. 4), a gene that is higher in the segmentation cascade in insects, including *D. melanogaster* [35], *T. castaneum* [36], *Nasonia vitripennis* [37], and *O. fasciatus* [38]. Lower imaging costs associated with cISH allowed us to obtain a time series tracking the appearance of each stripe of *Bg-hh* expression (Fig. 3), and HCR allowed us to observe the co-expression of both genes (Fig. 5). Shortly after head lobes become visible, *B. germanica hedgehog* (*Bg-hh*) expression appears (Fig. 3B, 5B). *Bg-hh* stripes appear one at a time, from anterior to posterior (Fig. 3B–H), although the timing of stripe appearance is not uniform. The antennal, mandibular, maxillary, labial, and first two thoracic segments appear rapidly and sequentially as the head lobes and germband condense (Fig. 5B, C). There is little detectable change in embryo morphology, as observed with DAPI stains, during the time these segments appear. Just before the two lateral plates of cells fuse in the head lobes, an eighth *Bg-hh* stripe (marking the third thoracic segment) appears (Fig. 5E). The embryo still shows eight *Bg-hh* stripes as the fusion process completes and the germband proper is formed (Fig. 5G).

We observed five *Bg-eve* stripes in an embryo shortly before *Bg-hh* appeared. These five stripes appear together in the middle of the anterior–posterior axis of the condensing germband, between the developing head

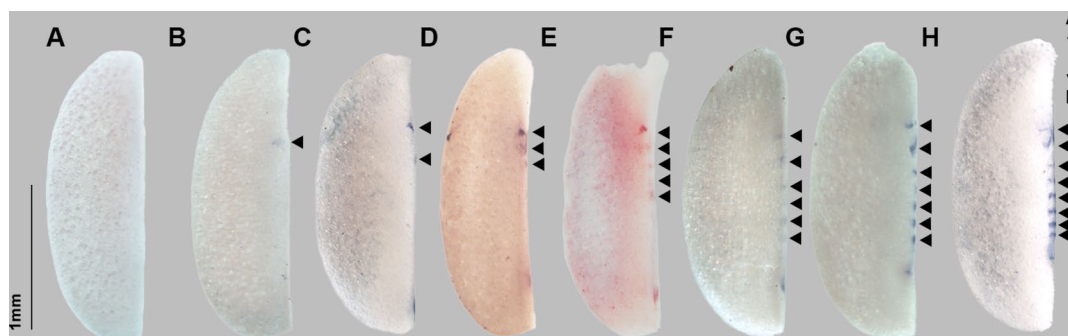


Fig. 3 Sequential appearance of gnathal and thoracic *Bg-hh* stripes in *B. germanica*. Chromogenic in situ for *Bg-hh*. The ventral side of the embryos faces right. Arrows indicate segments. Stripes of *Bg-hh* expression corresponding to each segment of the head and thorax appear individually. Dark spots at the posterior of embryos D–H may represent the posterior tissue that will ultimately form the segment addition zone

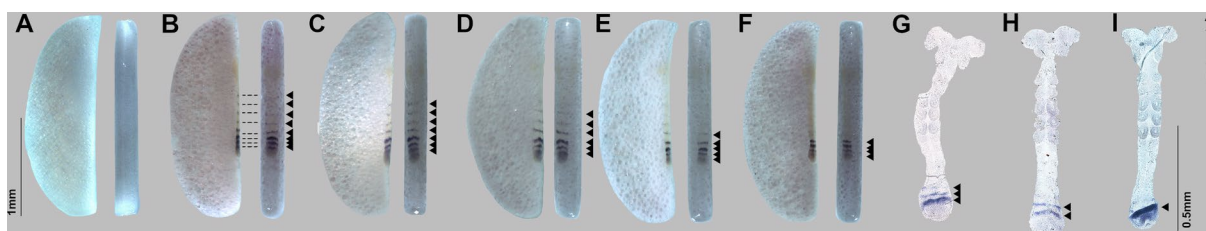


Fig. 4 *Bg-eve* stripes appear simultaneously and disappear sequentially. Chromogenic in situ of *even-skipped*. All embryos pictured are from the same ootheca. For each embryo, ventral view is shown on the right, lateral view is on the left, with the ventral side facing right. Dotted lines in B connect stripes of expression seen in the ventral and lateral views. Arrows highlight expression. Older embryos have fewer *even-skipped* stripes than younger embryos. *even-skipped* stripes associated with gnathal and thoracic segments are lighter in intensity than those associated with abdominal segments. Left scale for embryos A–F, right scale for embryos G–I

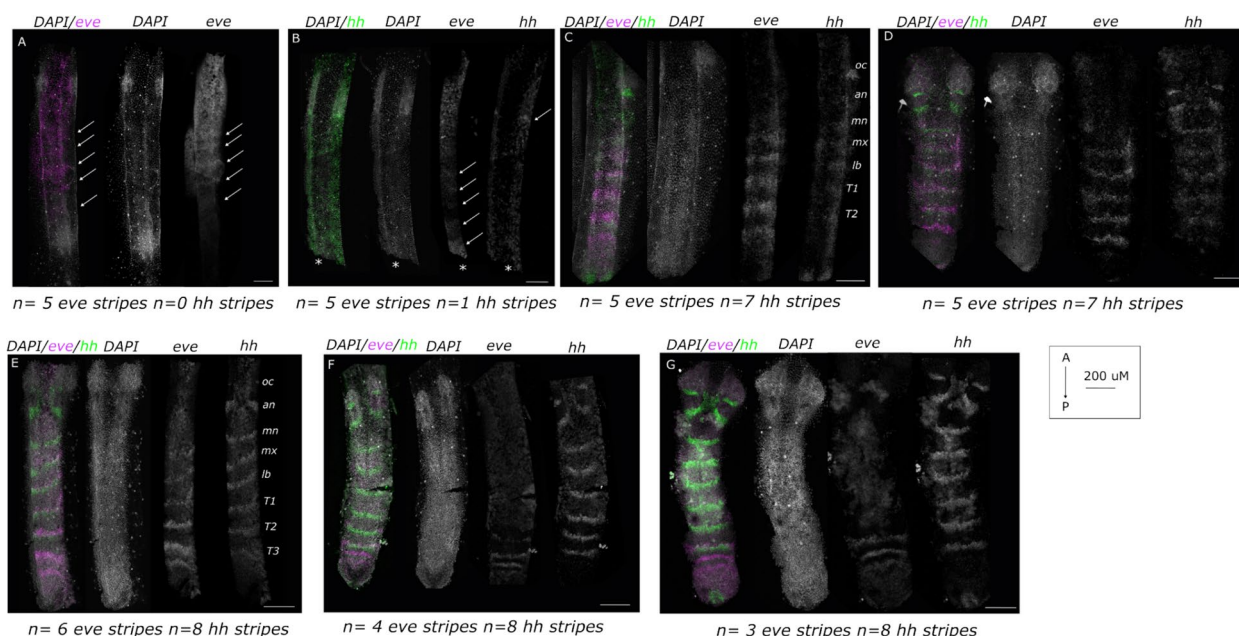


Fig. 5 Gnathal–thoracic segmentation. Patterns of *Bg-hh* and *Bg-eve* were observed with HCR during gnathal and thoracic segmentation (top panel). *Bg-eve* is shown in magenta, *Bg-hh* in green, and DAPI-stained nuclei in gray. Embryos are arranged from youngest (top left panel) to oldest (bottom right panel). The asterisk (*) in panel B indicates the embryo was broken at the posterior end. **A** *Bg-eve* expression appears before *Bg-hh* during stage 3 of germband formation. We observed 5 stripes of *Bg-eve* expression (white arrows) at this point. No signal was detected for *Bg-hh*. **B** The first *Bg-hh* stripes to appear are in the head lobe. At this point, there are still five *Bg-eve* stripes, although the initial expression of *Bg-hh* appears uncorrelated with *Bg-eve*. **C** and **D** Antennal through the second thoracic segment appears rapidly in the condensing germband, indicated by the jump from one to seven *Bg-hh* stripes with little to no change in embryo morphology. **E** The number of *Bg-eve* stripes increases from five to six as the number of *Bg-hh* stripes increases from seven to eight. **F, G** *Bg-eve* stripes gradually disappear as the number of *Bg-hh* stripes remains constant

lobes and what will become the segment addition zone (Fig. 4C, D, Fig. 5B, C). The five *Bg-eve* stripes persist as seven *Bg-hh* stripes appear, and they appear to mark the cells in the mandibular through the second thoracic segment. Note that pair-rule gene orthologs, such as *eve* are not known to be expressed in the pre-gnathal segments (ocular, antennal and intercalary) in any insects [39, 40]. As the anterior-most *Bg-eve* stripe disappears, a new *Bg-eve* stripe appears posterior to the rest (Fig. 5D).

This posterior-most stripe marks what will become the third and final thoracic segment. After *Bg-hh* expression appears in the third thoracic segment, we observed the number of *Bg-eve* stripes decline from six to three (Fig. 4D–G) as the number of *Bg-hh* stripes remains constant at eight (marking the ocular, mandibular and all gnathal and thoracic segments).

During abdominal segmentation, cells first express *Bg-eve* before expressing *Bg-hh*. *Bg-eve* expression fades

gradually in each segment as the *Bg-hh* expression strengthens (Fig. 6). *Bg-eve* stripes appear one by one from the posterior as they fade anteriorly, leaving a more or less constant number of three stripes in the anterior segment addition zone.

Axial patterning

The mRNA expression patterns of the homeobox transcription factor and posterior determinant *caudal* (*cad*), and the zinc-finger transcription factor and anterior determinant *hunchback* (*hb*) were used to observe the process of early axial patterning (i.e., determination of anterior and posterior of the embryo). Both genes are conserved blastoderm patterning genes in arthropods and Bilateria generally [34, 41]. In *B. germanica* embryos, cISH and HCR showed no *Bg-cad* or *Bg-hb* expression in the early blastoderm embryo (data not shown). This finding is corroborated by qPCR experiments (Fig. 7A), and suggests that *Bg-cad* and *Bg-hb* mRNA are not maternally deposited. Zygotic transcription of *Bg-hb* is initiated 2 days (8% development) post-ootheca extrusion. We observed a local peak of *Bg-hb* expression at 3 days (12% development) post-ootheca extrusion. *Bg-cad* expression initiates 3 days (12% development) post-ootheca extrusion and maintains its expression level throughout day 4. In the early germband stage of embryogenesis, HCR shows *Bg-cad* is expressed at the posterior end of the embryo (Fig. 7B). This broad domain of expression remains as the germband continues to elongate (Fig. 7B). Using HCR, no clear *Bg-hb* expression was observed at the early germband stage (Fig. 7B). Later, as the germband elongates, *Bg-hb* is expressed in paired lateral cells along the midline, and in a branching pattern into the head lobes.

Mesoderm formation

The bHLH encoding gene *twist* (*twi*) is a conserved myogenic and mesoderm marker within arthropods [20, 42–50] and in other bilaterians [47–50]. In insects, it also has a central role in the dorso-ventral patterning pathway [51–53]. We investigated the expression of *Bg-twi* from the blastoderm through to the germband stage in order to follow the initial stages of mesoderm formation. During the condensation of the germ anlage at the beginning of stage 3, a punctate pattern of expression can be seen on the posterior-ventral region (Fig. 8A–C). As the head lobes fuse in the germband (stage 4), *Bg-twi* is visible in the posterior germband and in the lateral head lobes, gradually expanding to cover almost the entire embryo (Fig. 8D–I). During posterior segmentation, *Bg-twi* expression remains in the limb-buds only, while a new expression pattern appears as segmental stripes in recently formed segments (Fig. 8J).

Discussion

We investigated the early stages in the embryonic development of the German cockroach, *Blattella germanica*, as an emerging model for evo-devo studies. *B. germanica* is a member of a basally branching taxon relative to the well-studied Holometabola, and its phylogenetic position in an underrepresented clade and in relation to other species studied can provide a key reference point for developmental studies. In this work, we have described some of the most fundamental developmental events in the earliest stages of development, including blastoderm and germband formation, cellularization, mesoderm formation, embryo polarization, and segmentation. We hope that these data will provide a developmental roadmap for *B. germanica*, highlighting unique aspects of its

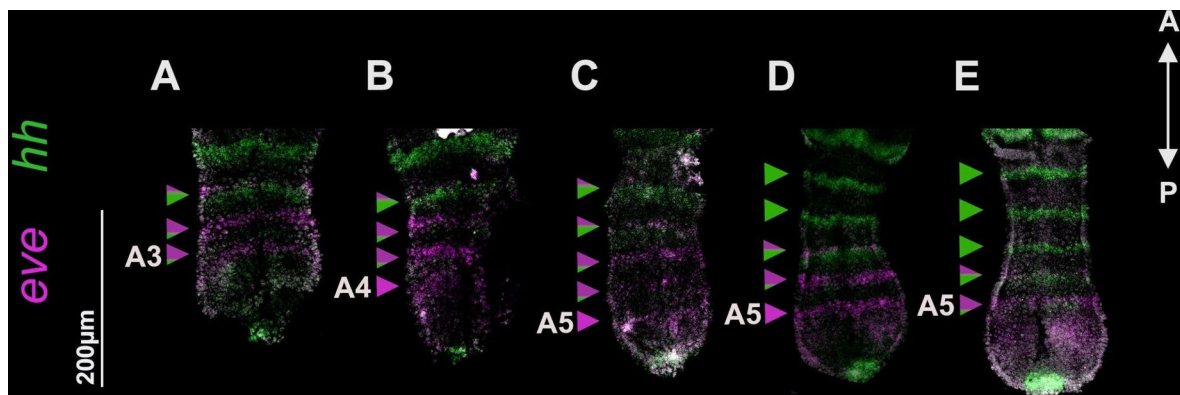


Fig. 6 Abdominal segmentation: during abdominal segmentation, *Bg-eve* stripes disappear as *Bg-hh* stripes appear. *Bg-eve* is shown in magenta and *Bg-hh* in green. Embryos are arranged from youngest (left) to oldest (right). Arrows to the left of the embryos highlight each stripe with a proportional representation of green or magenta to indicate how many cells in the stripe are expressing *Bg-eve* (magenta) versus *Bg-hh* (green). A3=abdominal segment 3, A4=abdominal segment 4, A5=abdominal segment 5

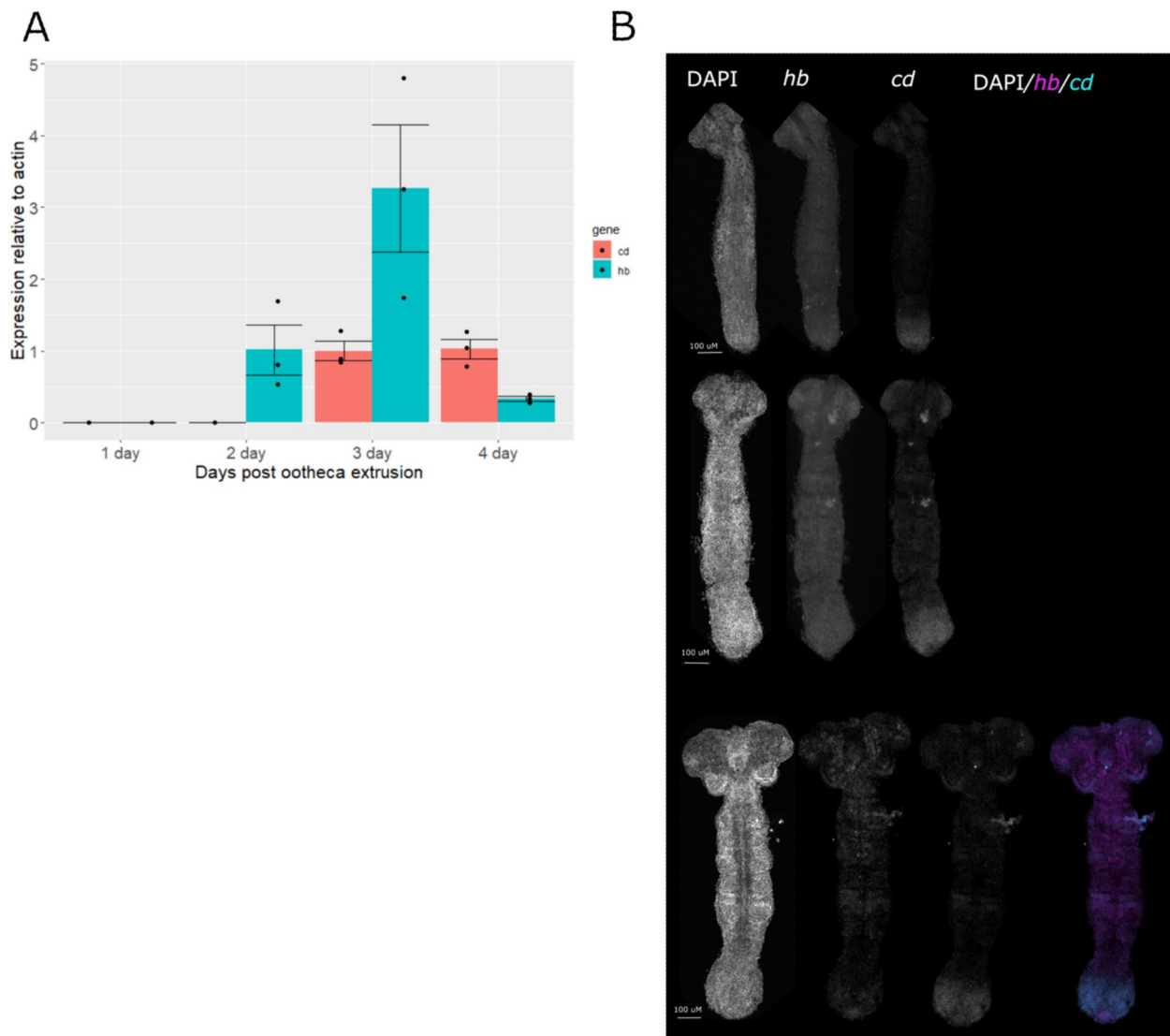


Fig. 7 Early expression of *hunchback* and *caudal*. **A** qPCR measuring *Bg-hb* and *Bg-cad* expression relative to actin levels in embryos from oothecae 1, 2, 3 and 4 days post-extrusion. *Bg-hb* expression peaks at 3 days (12% development) post-ootheca extrusion. **B** HCR of both genes in embryos 3 days post-extrusion. Embryos in top and middle row are approximately 4 days post-extrusion. Embryo in the bottom row shows neuronal expression of *Bg-hb* and is approximately 5 days post-extrusion

embryogenesis that can be compared to other insect species. Furthermore, we hope this study will stimulate additional research utilizing this emerging model organism.

The development of *Blattella germanica*

Early embryogenesis can be divided into four stages. Stage 1 involves cleavage and formation of a direct-differentiated blastoderm with nuclei migrating from the ventral to the dorsal surface. In stage 2, the syncytial blastoderm exhibits higher nuclear density ventrally compared to dorsally, suggesting nuclear migration. Cellularization occurs midway through this stage. Stage 3

sees the formation of a germ anlage/rudiment with larger polyploid nuclei dorsally, giving rise to serosa. Meanwhile, ventrally, the germ rudiment nuclei condense anteriorly, where head lobes will form. In stage 4, the germ rudiment's lateral plates fuse ventrally from posterior to anterior, forming the bipartite germband.

The anterior determinant *Bg-hb* and the posterior determinant *Bg-cad* are not expressed in early developmental stages, and only come up in the germband. This is contrary to what we had expected based on data from other species. However, in the milkweed bug *O. fasciatus*, as well as in the pea aphid *Acyrtosiphon pisum*

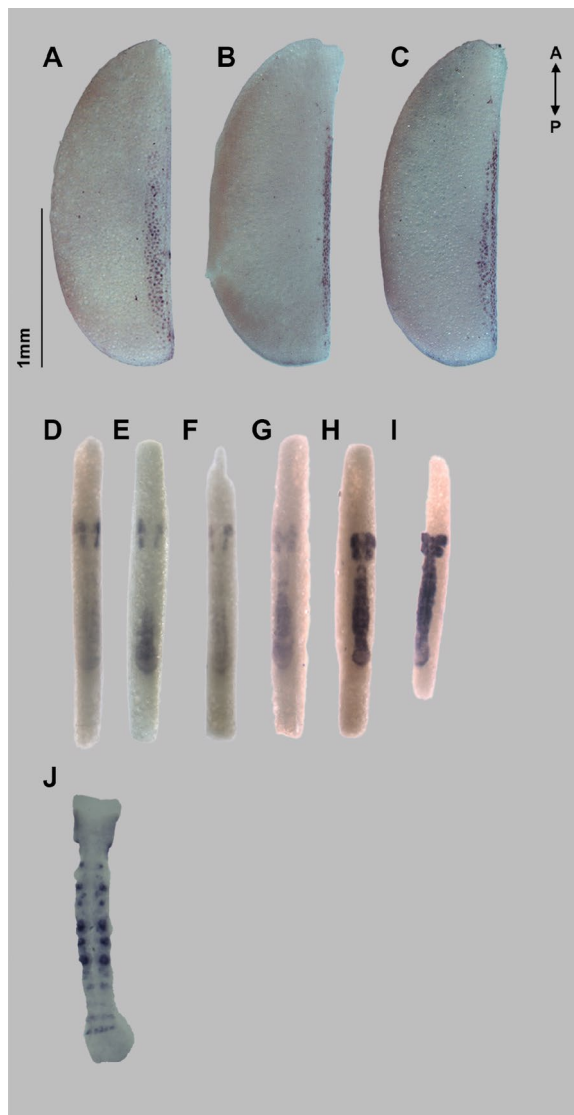


Fig. 8 Mesoderm formation. Chromogenic in situ of *Bg-twi*. All embryos in a row are from the same ootheca. **A–C** Germ rudiment (stage 3), embryos from lateral view are presented with the ventral side to the right. Individual cells marked as mesoderm are visible in a ventral position. Considering the unusual shape of the egg this is consistent with the classical expression pattern as seen in *D. melanogaster* [20] and *T. castaneum* [21]. **D–I** germband fusion through early germbands (stage 4 and on) ventral view of hacked eggs. The expression can be seen from the earliest stages in the presumptive head lobes and the posterior of the forming germband. The expression advances anteriorly with the fusion of the embryo proper. A clear patch is maintained for some time between the PGS and gnathal segments. **J** As limb primordia begin to form, *Bg-twi* becomes segmental and marks the formation of segmental mesoderm

(both members of Hemiptera), *cad* is not expressed maternally [54, 55]. Similarly, *hb* was not found to be significantly expressed in early stages of *O. fasciatus* [56]. Combined with our results in *B. germanica*, this

suggests that in hemimetabolous insects in general, and possibly ancestrally for insects, early polarization may not be driven by maternal transcription factors. Instead, it may be driven by structural elements related to the morphology of the egg.

We have not followed gastrulation and mesoderm formation in sufficient detail to draw strong conclusions about how they occur in *B. germanica*. However, the expression pattern of *Bg-twi* we do see is quite similar to that reported for the holometabolous beetle *T. castaneum* [21].

Segmentation in *B. germanica* follows the intermediate-germ paradigm. The determination of embryonic segments begins in stage 3, marked by the almost simultaneous segmentation of the pre-gnathal and gnatho-thoracic segments. During abdominal segmentation, *Bg-eve* precedes *Bg-hh* in each segment before fading as *Bg-hh* expression strengthens.

Evolutionary implications

Researchers in the early twentieth century (reviewed by [6, 18, 19]) discussed the formation of the insect blastoderm and noted two distinct phenomena during this phase. The first is the emergence pattern of nuclei on the egg's surface. This emergence can be uniform across the whole egg, as in *Oncopeltus fasciatus* (manuscript in preparation), or more concentrated on a specific region, usually the postero-ventral region, as in *B. germanica*. The second phenomenon is the final distribution of nuclei on the egg's surface. Following a local emergence, nuclei migrate across the surface and are eventually distributed uniformly, as in the cricket, *Gryllus bimaculatus* [57], or remain localized, as in *B. germanica*. Indeed, recent work has shown that even among species whose embryos all possess a uniform blastoderm phase, different processes control cell migration and nuclear division in this early stage [58]. Little work, though, has investigated the relationship between variation in blastoderm type—uniform versus direct-differentiated—and subsequent early germband patterning. For example, embryos with direct-differentiating blastoderms lose synchronous cleavage earlier than those with uniform blastoderms [6]. We found that the direct-differentiating blastoderm of *B. germanica* does not affect the expression patterns of the genes we studied. Most of the genes investigated in this paper were expressed in patterns similar to those previously reported in insects with uniform blastoderms. Preliminary results from a literature review (manuscript in preparation) suggest that the direct-differential blastoderm (regionalized emergence followed by regionalized final distribution) is an apomorphy of Polyneoptera.

Segmentation and tagmatization

The timing and dynamics of the segmentation process are summarized in Fig. 9. We have shown a transition in segmentation mode between the thoracic and abdominal segments during the development of *B. germanica*. At the level of segment-polarity genes, the process seems to be sequential throughout but more rapid in the early stages of segmentation. Looking at the expression of *Bg-eve* (a pair-rule gene in *Drosophila melanogaster*) representing a higher regulatory tier [34], it appears that the gnathal and thoracic segments exhibit a more-or-less simultaneous early determination phase, similar to the progressive segmentation described for the wasp *Nasonia vitripennis* [59], while the abdominal segments are patterned via a classical segment addition zone (SAZ) with a cycling process of segmentation, as shown in the holometabolous *Tribolium castaneum* [60, 61], the hemimetabolous *O. fasciatus* [30, 62] and several non-insect arthropods [63–65]. The distinction between the two segmentation modes is not as sharp as in *O. fasciatus*, where there is a transition from a blastoderm to an internalized germband between the two. However, gnatho-thoracic segmentation in *B. germanica* occurs within the early determined embryonic rudiment, whereas abdominal segmentation occurs from a posterior SAZ that is only formed towards the end of thoracic segmentation. The third thoracic segment is unusual in exhibiting a transitional mode. It is patterned later than the other thoracic segments but is still distinct from the SAZ-mediated patterning of the abdominal segments. This transition in segmentation dynamics between the thorax and the abdomen, similar to that reported in *O. fasciatus*, suggests that an early developmental boundary between these tagmata may be a more broadly conserved feature than previously recognized.

Follow-up experiments

We presented a rough time course of *Bg-twi* expression in the *B. germanica* embryo, but believe a more detailed time series would be valuable. Specifically, high resolution images combining *Bg-twi* probes with DAPI could illuminate how mesoderm formation proceeds as the lateral plates of the *B. germanica* embryo come together. Because the lateral plate model is a suggested apomorphy of Polyneoptera, understanding mesoderm formation in this type of embryo would be extremely valuable.

Materials and methods

Insect husbandry

The *Blattella germanica* colony was grown from several starting colonies supplied by Meital Labs (<https://www.meital-labs.co.il/>). Insects were kept at 25°C and ~40% humidity with a 14:10 D:L cycle. (Humidity and temperature values fluctuate by ~10% on a seasonal basis.) Insects were reared in large containers with perforated covers. Each container is 19×19x22 cm, with several dozen individuals of continuous generations. In the container, a few cardboard tubes were used as shelter. Insects were fed dog chow and dried oats ad libitum. Distilled water was provided in 50-ml Erlenmeyer flasks sealed with water-soaked cotton balls. The cages were cleaned, and the food and water were renewed weekly.

Embryo staging

As oothecae emerge from female *B. germanica*, the seam of the egg case is oriented dorsally (Fig. S3A). After all eggs are laid and the ootheca is fully extruded, it rotates 90 degrees, such that its seam is aligned laterally (Fig. S3C). We collected adult females laying eggs (identified by a partially extruded egg case), and we also collected females with oothecae that had extruded but were not rotated. A fully extruded but not rotated ootheca (Fig.

PGS	Ocular	hh	hh	hh	hh	hh	hh	hh	hh	hh	hh	hh	hh	hh	hh	hh	hh	hh	hh		
	Antennal	hh	hh	hh	hh	hh	hh	hh	hh	hh	hh	hh	hh	hh	hh	hh	hh	hh	hh		
Gnathal	Intercalary																				
	Mandibular	eve	eve	eve	eve+hh	eve+hh	eve+hh	eve+hh	eve+hh	hh	hh	hh	hh	hh	hh	hh	hh	hh	hh		
	Maxillary	eve	eve	eve	eve	eve+hh	eve+hh	eve+hh	eve+hh	eve+hh	hh	hh	hh	hh	hh	hh	hh	hh	hh		
Thorax	Labial	eve	eve	eve	eve	eve	eve+hh	eve+hh	eve+hh	eve+hh	eve+hh	hh	hh	hh	hh	hh	hh	hh	hh		
	T1	eve	eve	eve	eve	eve	eve	eve+hh	eve+hh	eve+hh	eve+hh	hh	hh	hh	hh	hh	hh	hh	hh		
	T2	eve	eve	eve	eve	eve	eve	eve	eve+hh	eve+hh	eve+hh	hh	hh	hh	hh	hh	hh	hh	hh		
	T3									eve+hh	eve+hh	eve+hh	eve+hh	eve+hh	hh	hh	hh	hh	hh		
Abdomen	A1								eve	eve	eve	eve	eve	eve	hh	hh	hh	hh	hh		
	A2											eve	eve	eve	hh	hh	hh	hh	hh		
	A3												eve	eve	eve	hh	hh	hh	hh		
	A4													eve	eve	eve	hh	hh	hh		
	A5														eve	eve	eve	hh	hh		
	A6															eve	eve	eve	hh		
	A7																eve	eve	eve		
	A8																	eve	eve		
Step		1	2	3	4	5	6	7	8	10	11	12	13	14	15	16	17	18	19	20	
		Gnathal+T1-2 segmentation								T3 segmentation			Abdominal segmentation								

Fig. 9 Segmentation dynamics. Summary of *Bg-eve* and *Bg-hh* expression data over time. Each row represents a segment, with the columns representing successive time-points (steps) in the developmental process. The steps are arbitrary points in which there is a change in expression pattern relative to the previous step, and are not to scale. Data accumulated from numerous single- and double-stained embryos, not all of which are shown in the Results

S3B) was set as time point 0. Since the oothecae are not viable after being removed from the mother, collected females were isolated until their embryos had reached the desired age, at which point we manually removed the oothecae for further study.

Egg case removal and fixation

Staged females were anesthetized with CO₂ or cooled on ice before manual removal of oothecae. Oothecae were placed into 1 mL of water, then heated for 10 min at 85°C and subsequently submerged in ice for up to five min. Except for embryos used for wheat germ agglutinin (WGA) staining, embryos were dissected out of the ootheca in phosphate-buffered saline with Tween (PBST) and placed directly into fixative (4% formaldehyde in phosphate-buffered saline). Embryos were fixed in 4% formaldehyde for one hour and then gradually dehydrated to 100% methanol. Embryos were stored in methanol at -20°C for at least overnight, up to several months. For some nuclear stains and immunohistochemistry, the methanol step was skipped. For embryos used in WGA staining, dissection was done in phosphate-buffered saline with no detergent, and fixation was performed for 20 min in 4% paraformaldehyde in phosphate-buffered saline.

Nuclear staining

If necessary, embryos were rehydrated gradually from methanol and washed for an additional 5 min in PBST. Fixed embryos were stained with Sytox green (1:2000; Invitrogen, Sytox Green Nucleic acid, S7020) in 1 mL PBST and incubated at RT, in the dark, for 20 min. Stained embryos were washed twice in the dark for three min with PBST solution. When staining with DAPI, we added DAPI (1:1000; Invitrogen, DAPI, D1306) in 1 mL PBST and incubated at RT in the dark for 15 min. Stained embryos were washed once for 15 min with PBST in the dark. Stained embryos were imaged as described below and the “Find Maxima” tool in FIJI software was used to manually count nuclei. Embryos were inspected to ensure the maxima identified by the software corresponded to nuclei with no false positives or false negatives.

Immuno-fluorescence

Before adding primary antibodies, the embryos were incubated in a blocking solution (1% bovine serum albumin (MP Biomedicals cat no. 160069) and 5% NGS (normal goat serum, Vector Labs cat no. S-1000) in PBST) for one hour. Embryos were incubated with anti-phosphorylated histone H3 (PH3) antibody (1:500; Abcam, ab14955) overnight. The following morning, embryos were washed four times for 15 min with PBST. Secondary antibodies (1:200; Alexa Fluor 448/546/594, anti-mouse, Invitrogen)

were added to the blocking solution, and embryos were incubated in the dark for 2 h.

Gene sequence isolation

All gene sequences were identified in tBLASTn searches of *B. germanica* gene models on the i5k database (bger_OGS_v1.2, url: https://i5k.nal.usda.gov/data/Arthropoda/blager-%28Blattella_germanica%29/Bger_2.0/2.Official%20or%20Primary%20Gene%20Set/). *Bg-hh* (BGER011018-RA-CDS) was identified after a tBLASTn search using Hedgehog protein from *O. fasciatus* (NCBI accession number AYR04649.1) as bait. *Bg-hb* (gene model BGER015825-RA-CDS) was identified in a tBLASTn search using the Hunchback protein from *D. melanogaster* as bait (Fly Base FBgn0001180). *Bg-cad* (gene model BGER016043-RA-CDS) was identified using Caudal protein from *D. melanogaster* as bait (Fly Base FBgn0000251). *Bg-twi* (gene model BGER025575-RA-CDS) was identified using *D. melanogaster* Twist protein (Fly Base FBgn0003900) as bait. *Bg-eve* was identified using an *even-skipped* sequence from *Drosophila melanogaster* as bait (Fly Base FBgn0000606). The *B. germanica* gene model retrieved as a top hit in a tBLASTn search for *eve* (BGER013241-RA-CDS) was only 166 amino acids. When aligned to other insect Even-skipped proteins, this *B. germanica* gene model was missing sequence from the C-terminal end. We then used a sequence from the *Cryptotermes secundus* Even-skipped protein (XP_023719287.1) as bait in a tBLASTn search of the *B. germanica* genome in an attempt to retrieve sequence from exons downstream of the *B. germanica* gene model with the putative *eve* sequence. This strategy was successful; we obtained what appeared to be a 317 bp exon downstream of the original *B. germanica* gene model. Using this exon as a template for a reverse primer and the gene model (BGER013241-RA-CD) as a template for a forward primer, we designed primers that then amplified a 916 bp fragment of *B. germanica even-skipped* from embryonic cDNA. This sequence was deposited in NCBI with the accession numbers PQ505666 and PQ505667.

Chromogenic in situ hybridization probe preparation

We collected total RNA from 3-day-old oothecae manually removed from the female. RNA was extracted with Trizol (Invitrogen cat no. 15596026) using the manufacturer's protocol. One microgram of RNA was used in a reverse transcription reaction primed with a 1:1 mixture of oligo dT:random hexamers. We used Bioline's RTase (cat No BiO-27036). Templates for *Bg-hh*, *Bg-eve*, *Bg-hb*, *Bg-cad*, and *Bg-twi* probes were amplified using Tiger polymerase from Hylabs (EZ-2031), with primers that had a T7 sequence added to the 5' end of the reverse primer. To amplify templates for the *Bg-hh* probe, we

used the following cycling parameters: 95°C for 3 min, followed by 32 cycles of 95°C for 30 s, 55°C for 30 s, and 72°C for 30 s, with a 3-min extension at 72°C at the end of the cycles. Other probes were amplified with the same cycling parameters but different annealing temperatures (see PCR conditions table) Templates were purified using Macherey–Nagel’s NucleoSpin Gel and PCR Clean-up kit (740,609.50). We synthesized DIG-labeled probes with T7 polymerase from Roche (10,881,767,001).

Chromogenic in situ hybridization

Embryos were gradually rehydrated from 100% methanol. After 3 × 1-min PBST washes, a post-fixation of 20 min in 4% formaldehyde in PBST and another round of 3 × 1-min PBST washes were carried out. Embryos were incubated in a hybridization buffer at 65 °C for 5 min, then the hybridization buffer was refreshed, and embryos were incubated again in a hybridization buffer at 65 °C for 2–4 h. DIG-labeled probes were applied at a 1 ng/μL concentration in the hybridization buffer and left overnight at 65 °C. The following day, the following washes were performed: 20 min in preheated hyb buffer (65 °C); 3 × 20 min in 2×SSC/0.1% Tween-20 (65 °C); 3 × 20 min in 0.2×SSC/0.1% Tween-20 (65 °C); 2 × 10 min in PBST at room temp; 1 h in blocking solution (5% sheep or goat serum, 2 mg/mL BSA, 1% DMSO in PBST); 4 h in 1:1500 solution of anti-digoxigenin antibody (Roche, cat no. 11333089001):blocking solution; 3 × 1-min PBST washes, and left overnight in PBST at 4 °C. The following day, embryos were washed in the following series: 4 × 20 min wash in PBST; 2 × 10 min of washing in freshly prepared staining solution (0.1 M 9.5 Tris–HCl; 0.05M MgCl₂; 0.1M NaCl; 0.1M Tween-20); 1 × 10 min of staining solution + PVA (0.1 M 9.5 Tris–HCl; 0.05M MgCl₂; 0.1M NaCl; 0.1M Tween-20; 0.025% polyvinyl alcohol). 20 μL of NBT/BCIP from Roche in 980 μL of staining solution + PVA was used for color development, which continued up to 4 h. Staining reactions were stopped when we observed background stain developing. Staining reactions were stopped with PBST washes and fixation in 50% methanol:PBST. Embryos were imaged in 70% glycerol.

Hybridization chain reaction

We used probes designed by Molecular Instruments for *Bg-cad* (lot number PRP735), *Bg-hb* (lot number PRP734), *Bg-hh* (lot number PRK420), *Bg-eve* (lot number PRK419), and *Bg-twi* (lot number RTG920). For probe design, we provided Molecular Instruments with the entirety of each gene’s available coding sequence. Probes designed by Molecular Instruments target several dozen nucleotides each and span the entirety of the coding sequence in a non-contiguous fashion. Probes for

Bg-hb and *Bg-hh* were all designed to anchor an amplification reaction with a 488 fluorophore. Probes for *Bg-eve*, *Bg-cad*, and *Bg-twi* were designed to anchor an amplification reaction with a 594 fluorophore.

For HCR-RNA FISH, a modified version of the protocol described by Bruce et al. [66] was used. Hybridization buffer, wash buffer, and amplification buffer were provided by Molecular Instruments, while we made the detergent solution (1% SDS, 0.5% Tween, 50 mM Tris–HCl (pH 7.5), 1 mM EDTA (pH 8.0), 150 mM NaCl) as described by Bruce et al. [66]. Embryos were rehydrated from methanol to PBST as described above in the chromogenic in situ section and then washed 1 × 10 min and 2 × 5 min in PBST. Embryos were incubated at RT for 30 min in the detergent solution, then 30 min at 37 °C in 200 μL of hybridization buffer. Probes were prepared at a concentration of approximately 10 nM, made by diluting 1.6 μL of the 1 μM stock from Molecular Instruments into 150 μL of hybridization buffer. Embryos were incubated overnight at 37 °C in the probe solution. The following day, embryos were washed in 1 mL of wash buffer at 37 °C (4 × 15 min), followed by 2 × 5-min washes at RT with 5% SSCT (5×sodium chloride sodium citrate with 1% Tween). Embryos were incubated in an amplification buffer (Molecular Instruments) for 30 min at RT, while hairpins were prepared by heating to 95 °C for 30 seconds, followed by 30 min at RT in the dark. 4 μL of each hairpin were added to 100 μL of the amplification buffer. This solution was applied to embryos after removing the 1 mL of the amplification buffer used for the pre-amplification step. Embryos were then incubated overnight in the dark at RT. Embryos were washed the next morning with 5% SSCT washes at RT (volume 1 mL) twice for 5 min and once for 15 min. We then did a 15-min wash with 1 μL DAPI into 1 mL of 5% SSCT, followed by two 15-min washes with 5% SSCT. Embryos were placed in 50% glycerol/PBS for 30 min before being transferred to 70% glycerol in PBS and mounted on slides.

Wheat germ agglutinin staining

Immediately after a 20-min fix in 4% paraformaldehyde, embryos were washed for 3×5 min in phosphate-buffered saline (PBS). Embryos were then transferred to WGA (Invitrogen, Wheat Germ Agglutinin (WGA), W21405) in PBS (1 ng/mL) and incubated for thirty min. Embryos were then washed for 3×10 min in phosphate-buffered saline, with the second wash containing DAPI at a concentration of 5 ng/mL. Embryos were mounted and visualized in 70% glycerol.

qPCR

Embryos were boiled and dissected in PBST as described above: “Egg case removal and fixation”. Upon dissection,

Embryos were immediately placed in Trizol. A single sample contained all embryos from one ootheca. RNA was extracted according to the manufacturer's protocol. Two hundred to three hundred nanograms of RNA were put into a reverse transcription reaction. Watchmaker StellarScript reverse transcriptase was used to generate cDNA, with the following parameters used in the thermocycler: 25°C for 10 min, 42°C for 20 min, and then 80°C for 10 min. qPCR primers were designed to span exon junctions or in two separate exons. Primer efficiency was validated with a dilution series. qPCR was performed on QuantStudio3 from ThermoFisher using Fast SYBR Green Master Mix (Cat no 4385610) in 10- μ L reactions. All reactions were performed using technical triplicates. Each biological replicate contained all the RNA from a single ootheca. We ran *cyclophilin* and *actin* as internal controls for each biological sample; however, we could not amplify cyclophilin in 1- and 2-day-old oothecae. We used the Pfaffl method [67] to normalize expression values of *caudal* and *hunchback* to the geometric mean of *actin* and *cyclophilin* expression for samples from 3 and 4-day-old oothecae. We calculated expression of each individual biological replicate relative to the mean for a specific treatment and gene, using $E^{\Delta\Delta Ct}$, where E = empirically determined amplification efficiency for a primer set, and $\Delta\Delta Ct$ is the difference between the mean Ct of all biological replicates and the mean Ct of technical replicates for a given biological replicate. We then made a ratio of relative expression for a target gene/geometric mean of the relative expressions for both cyclophilin and actin.

We then re-ran the analysis, normalizing *caudal* and *hunchback* expressions to *actin* alone. The changes were not significant when expression of *caudal* and *hunchback* were normalized to *actin* alone, so we proceeded to use only *actin* for further analysis so that 3 and 4-day samples could be compared to samples from 1 and 2-day-old oothecae.

Imaging

Egg case and embryo dissections were done under a 2000-Stem ZEISS dissecting scope. All embryos were mounted and imaged in 70% glycerol in PBT.

Images of ISH and IF stained embryos were captured using a Nikon 'digital sight' console connected to a DS-Fi1 digital camera mounted on either an SMZ1500 Nikon dissecting scope or an AZ100 zoom stereoscope. Images of slide-mounted embryos were captured with the same console and camera mounted on an Eclipse 80i Nikon Microscope.

HCR images were acquired with an Olympus FV1200 confocal based on an IX-83 inverted microscope

(Olympus, Japan), using a 10x/0.4 or 40x/0.95 air objective. Confocal fluorescence images of DAPI, Alexa 488 anti-PH3, Alexa 488 anti-alpha tubulin, and DIC images were acquired. The DAPI channel used 405 nm excitation and a 430–470 nm emission, and the Alexa 488 channel used 488 nm excitation and a 500–540 nm emission, acquired sequentially. Z- Z-stacks were acquired with 1.5- or 4- μ m stepping.

Images were processed in Fiji (Fiji is just ImageJ) [68]. We selected and projected the Z-stacks containing the signal for each fluorescent channel, as determined subjectively by the eye. After projecting stacks, we adjusted the contrast and brightness of each channel (using the window, level, contrast, and brightness scales in Fiji) to maximize the signal from the HCR. We then false-colored and merged channels.

Supplementary Information

The online version contains supplementary material available at <https://doi.org/10.1186/s13227-024-00234-2>.

Supplementary file 1: Supplemental Figure 1: Cell division becomes restricted to the ventral side of the egg after the formation of the germ rudiment. DAPI (blue) and anti-phospho-histone H3 (green) mark nuclei and dividing cells in embryos stage 1-4. Cell division is observed across the surface of the egg in embryonic stages 1 and 2 (panels A-C), but once the germ rudiment forms, cell division occurs overwhelmingly in the area of the forming germband (panels D-H).

Supplementary file 2: Supplemental Figure 2: Representative images from 4 different embryos from the same egg case taken 24 hours post extrusion (4% of developmental time). Only the embryo in B shows a discernable signal of WGA staining around nuclei which is distinct from the background.

Supplementary file 3: Supplemental Figure 3: Ootheca protrusion in the German Cockroach female. (A) As the egg case protrudes from the posterior abdomen of the female, the seam of the egg case is oriented dorsally. Eggs are laid successively into individual compartments. (B) After all eggs are laid and the ootheca is fully extruded, the female rotates it 90 degrees, such that its seam is aligned laterally (C).

Supplementary file 4: Supplementary table 1: Primers and PCR conditions for gene cloning.

Acknowledgements

We are grateful to Dr. Naomi Melamed-Book from the Bioimaging facility of the Institute of Life Sciences at the Hebrew University for help with confocal imaging, and to Mira Cohen for general technical support.

Author contributions

ABLV, JRW and OMLA did experiments and generated data. ABLV and JRW wrote the first draft of the paper and prepared the figures. ABLV, JRW and ADC finalized the manuscript. JRW provided supervision for ABLV and OMLA. ADC provided general project supervision and acquired funding.

Funding

This work was funded by the Israel Science Foundation grant #570/21. JRW was supported by a Zuckerman foundation post-doctoral fellowship.

Data availability

No datasets were generated or analysed during the current study.

Declarations

Ethics approval and consent to participate

The authors declare that they have no ethical issues to disclose.

Consent for publication

All of the co-authors have read the manuscript and give their consent to its publication.

Competing interests

The authors declare no competing interests.

Received: 9 July 2024 Accepted: 18 October 2024

Published online: 26 October 2024

References

- Belles X, Maestro JL, Piulachs M-D. The German cockroach as a model in insect development and reproduction in an endocrine context. In: Jurenka R, editor. *Advances in insect physiology*. Cham: Academic Press; 2024. p. 1–47.
- Cruz J, Maestro O, Franch-Marro X, Martín D. Nuclear receptors EcR-A/RXR and HR3 control early embryogenesis in the short-germ hemimetabolous insect *Blattella germanica*. *iScience*. 2023;26:106548. <https://doi.org/10.1016/j.isci.2023.106548>.
- Tanaka A. Stages in the embryonic development of the German cockroach, *Blattella germanica*. *Kontyu*. 1976;44:512–25.
- Wexler J, Pick L, Chipman A. Segmental expression of two ecdysone pathway genes during embryogenesis of hemimetabolous insects. *Dev Biol*. 2023;498:87–96. <https://doi.org/10.1016/j.ydbio.2023.03.008>.
- Bell WJ, Roth LM, Nalepa CA. Reproduction. In: Bell WJ, editor. *Cockroaches ecology, behavior and natural history*. New York: Johns Hopkins University Press; 2007. p. 116–30.
- Anderson D. The development of hemimetabolous insects. In: Counce SJ, Waddington CH, editors. *Developmental systems: insects*. Academic Press; 1972. p. 95–163.
- Eastham L. A contribution to the embryology of *Pieris rapae*. *J Cell Sci*. 1927;52–71:353–94. <https://doi.org/10.1242/jcs.52-71.283.353>.
- Nagy L, Riddiford L, Kiguchi K. Morphogenesis in the early embryo of the lepidopteran *Bombyx mori*. *Dev Biol*. 1994;165:15.
- Heider K. Die embryonalentwicklung von *Hydrophilus piceus* L. Verlag von Gustav Fischer. 1889.
- Paterson NF. Observations on the embryology of *Corynodes pusis* (Coleoptera, Chrysomelidae). *J Cell Sci*. 1935;78:43.
- Paterson NF. A contribution to the embryological development of *Euryope terminalis* Baly, (Coleoptera, Phytophaga, chrysomelide.) Part I: the early embryological development. *S Afr J Sci*. 1931;28:344–311.
- Sarashina I, Mito T, Saito M, Uneme H, Miyawaki K, Shinmyo Y, Ohuchi H, Noji S. Location of micropyles and early embryonic development of the two-spotted cricket *Gryllus bimaculatus* (Insecta, Orthoptera). *Dev Growth Differ*. 2005;47:99–108. <https://doi.org/10.1111/j.1440-169x.2005.00786.x>.
- Sauer HW. Zeitraffer-Mikro-Film-Analyse Embryonaler Differenzierungsphasen Von *Gryllus Domesticus*. *Z Morphol Okol Tiere*. 1966;56:143–251.
- Tanigawa N, Matsumoto K, Yasuyama K, Numata H, Shiga S. Early embryonic development and diapause stage in the band-legged ground cricket *Dianemobius nigrofasciatus*. *Dev Genes Evol*. 2009;219:589–96. <https://doi.org/10.1007/s00427-010-0320-x>.
- Mtow S, Machida R. Egg structure and embryonic development of arctoperlarian stoneflies: a comparative embryological study (Plecoptera). *Arthropod Syst Phylogeny*. 2018;76:22.
- Fujita M, Machida R. Embryonic development of *Eucoyrdia yasumatsui* Asahina, with special reference to external morphology (Insecta: Blattodea, Corydiidae). *J Morphol*. 2017;278:1469–89. <https://doi.org/10.1002/jmor.20725>.
- Shimizu S, Machida R. Development and reproductive biology of Dermaptera: a comparative study of thirteen species from eight families. *Arthropod Syst Phylogeny*. 2024;82:35–75.
- Eastham LES. The formation of germ layers in insects. *Biol Rev*. 1930;5:1–29. <https://doi.org/10.1111/j.1469-185X.1930.tb00891.x>.
- Johannsen OA, Butt FH. Embryology of insects and myriapods; the developmental history of insects, centipedes, and millepedes from egg deposition [!] to hatching. New York: McGraw-Hill Book Company, inc; 1941. <https://doi.org/10.5962/bhl.title.6583>.
- Leptin M. *twist* and *snail* as positive and negative regulators during *Drosophila* mesoderm development. *Genes Dev*. 1991;5:1568–76. <https://doi.org/10.1101/gad.5.9.1568>.
- Handel K, Basal A, Fan X, Roth S. *Tribolium castaneum twist*: gastrulation and mesoderm formation in a short-germ beetle. *Dev Genes Evol*. 2005;215:13–31. <https://doi.org/10.1007/s00427-004-0446-9>.
- Donoughe S, Extavour CG. Embryonic development of the cricket *Gryllus bimaculatus*. *Dev Biol*. 2016;411:140–56. <https://doi.org/10.1016/j.ydbio.2015.04.009>.
- Ullmann SL. The origin and structure of the mesoderm and the formation of the coelomic sacs in *Tenebrio molitor* L. [Insecta, Coleoptera]. *Philosophical Transactions of the Royal Society of London. Series B Biol Sci*. 1964;248:245–77.
- Pechmann M, Kenny NJ, Pott L, Heger P, Chen Y-T, Buchta T, Özüak O, Lynch J, Roth S. Striking parallels between dorsoventral patterning in *Drosophila* and *Gryllus* reveal a complex evolutionary history behind a model gene regulatory network. *eLife*. 2021;10:e68287. <https://doi.org/10.7554/eLife.68287>.
- Fujita M, Lee C-Y, Machida R. Reproductive biology and embryonic development of *Nocticola* sp. (Blattodea: Nocticolidae). *Arthropod Syst Phylogeny*. 2020;78:393–403.
- Panfili KA. Extraembryonic development in insects and the acrobatics of blastokinesis. *Dev Biol*. 2008;313:471–91. <https://doi.org/10.1016/j.ydbio.2007.11.004>.
- Tang Q, Vargo EL, Ahmad I, Jiang H, Varadinová ZK, Dovih P, et al. Solving the 250-year-old mystery of the origin and global spread of the German cockroach, *Blattella germanica*. *Proc Natl Acad Sci*. 2024;121:e2401185121.
- Shirai Y, Piulachs M-D, Belles X, Daimon T. DIPA-CRISPR is a simple and accessible method for insect gene editing. *Cell Rep Methods*. 2022;2:100215. <https://doi.org/10.1016/j.crmeth.2022.100215>.
- Stahi R, Chipman AD. Blastoderm segmentation in *Oncopeltus fasciatus* and the evolution of insect segmentation mechanisms. *Proc R Soc B*. 2016;283:20161745. <https://doi.org/10.1098/rspb.2016.1745>.
- Auman T, Vreede BMI, Weiss A, Hester SD, Williams TA, Nagy LM, Chipman AD. Dynamics of growth zone patterning in the milkweed bug *Oncopeltus fasciatus*. *Development*. 2017;144:1896–905. <https://doi.org/10.1242/dev.142091>.
- Truckenbrodt W. Über die Entstehung der Serosa im besamten und im unbesamten Ei von *Odontotermes badius* Hav. (Insecta, Isoptera). *Zeitschrift für Morphologie der Tiere*. 1973; 76, 16.
- Panfili KA, Liu PZ, Akam M, Kaufman TC. *Oncopeltus fasciatus zen* is essential for serosal tissue function in katatrepsis. *Dev Biol*. 2006;292:226–43. <https://doi.org/10.1016/j.ydbio.2005.12.028>.
- Panfili KA, Oberhofer G, Roth S. High plasticity in epithelial morphogenesis during insect dorsal closure. *Biology Open*. 2013;2:1108–18. <https://doi.org/10.1242/bio.20136072>.
- Chipman AD. The evolution of the gene regulatory networks patterning the *Drosophila* blastoderm, current topics in developmental biology. Amsterdam: Elsevier; 2020. p. 297–324. <https://doi.org/10.1016/bs.ctdb.2020.02.004>.
- Macdonald PM, Ingham P, Struhl G. Isolation, structure, and expression of *even-skipped*: a second pair-rule gene of *Drosophila* containing a homeo box. *Cell*. 1986;47:721–34. [https://doi.org/10.1016/0092-8674\(86\)90515-5](https://doi.org/10.1016/0092-8674(86)90515-5).
- Brown SJ, Parrish JK, Beeman RW, Denell RE. Molecular characterization and embryonic expression of the *even-skipped* ortholog of *Tribolium castaneum*. *Mech Dev*. 1997;61:165–73. [https://doi.org/10.1016/s0925-4773\(96\)00642-9](https://doi.org/10.1016/s0925-4773(96)00642-9).
- Rosenberg MI, Brent AE, Payre F, Desplan C. Dual mode of embryonic development is highlighted by expression and function of *Nasonia* pair-rule genes. *Elife*. 2014;3: e01440. <https://doi.org/10.7554/eLife.01440>.
- Liu PZ, Kaufman TC. Short and long germ segmentation: unanswered questions in the evolution of a developmental mode. *Evol Dev*. 2005;7:629–46. <https://doi.org/10.1111/j.1525-142X.2005.05066.x>.

39. Posnien N, Bucher G. Formation of the insect head involves lateral contribution of the intercalary segment, which depends on *Tc-labial* function. *Dev Biol.* 2010;338:107–16. <https://doi.org/10.1016/j.ydbio.2009.11.010>.
40. Lev O, Chipman AD. Development of the pre-gnathal segments in the milkweed bug *Oncopeltus fasciatus* suggests they are not serial homologs of trunk segments. *Front Cell Dev Biol.* 2021;9: 695135.
41. Auman T, Chipman AD. The evolution of gene regulatory networks that define arthropod body plans. *Integr Comp Biol.* 2017;57:523–32. <https://doi.org/10.1093/icb/ix035>.
42. Baylies MK, Bate M. *twist*: A myogenic switch in *Drosophila*. *Science.* 1996;272:1481–4. <https://doi.org/10.1126/science.272.5267.1481>.
43. Castanon I, Baylies MK. A Twist in fate: evolutionary comparison of Twist structure and function. *Gene.* 2002;287:11–22. [https://doi.org/10.1016/S0378-1119\(01\)00893-9](https://doi.org/10.1016/S0378-1119(01)00893-9).
44. Price AL, Patel NH. Investigating divergent mechanisms of mesoderm development in arthropods: the expression of *Ph-twist* and *Ph-mef2* in *Parhyale hawaiiensis*. *J Exp Zool B.* 2008;310B:24–40. <https://doi.org/10.1002/jez.b.21135>.
45. Sommer RJ, Tautz D. Expression patterns of *twist* and *snail* in *Tribolium* (Coleoptera) suggest a homologous formation of mesoderm in long and short germ band insects. *Dev Genet.* 1994;15:32–7. <https://doi.org/10.1002/dvg.1020150105>.
46. Yamazaki K, Akiyama-Oda Y, Oda H. Expression patterns of a *twist*-related gene in embryos of the spider *Achaearanea tepidariorum* reveal divergent aspects of mesoderm development in the fly and spider. *Zool J Linn Soc.* 2005;22:10. <https://doi.org/10.2108/zsj.22.177>.
47. Brand C, Bergter A, Paululat A. Cloning of a *twist* orthologue from *Enchytraeus coronatus* (Annelida, Oligochaeta). *DNA Seq.* 2003;14:25–31. <https://doi.org/10.1080/1042517021000050552>.
48. Dill KK, Thamm K, Seaver EC. Characterization of *twist* and *snail* gene expression during mesoderm and nervous system development in the polychaete annelid *Capitella* sp. I. *Development Genes and Evolution.* 2007;217:435–47. <https://doi.org/10.1007/s00427-007-0153-4>.
49. Gitelman I. Twist protein in mouse embryogenesis. *Dev Biol.* 1997;189:205–14. <https://doi.org/10.1006/dbio.1997.8614>.
50. Hopwood ND, Pluck A, Gurdon JB. A *Xenopus* mRNA related to *Drosophila twist* is expressed in response to induction in the mesoderm and the neural crest. *Cell.* 1989;59:893–903. [https://doi.org/10.1016/0092-8674\(89\)90612-0](https://doi.org/10.1016/0092-8674(89)90612-0).
51. Brown SJ, Denell RE. Segmentation and dorsoventral patterning in *Tribolium*. *Semin Cell Dev Biol.* 1996;7:553–60. <https://doi.org/10.1006/scdb.1996.0069>.
52. Jiang J, Kosman D, Ip YT, Levine M. The *dorsal* morphogen gradient regulates the mesoderm determinant *twist* in early *Drosophila* embryos. *Genes Dev.* 1991;5:1881–91. <https://doi.org/10.1101/gad.5.10.1881>.
53. Lynch JA, Roth S. The evolution of dorsal–ventral patterning mechanisms in insects. *Genes Dev.* 2011;25:13.
54. Chang C, Hsiao Y, Huang T-Y, Cook CE, Shigenobu S, Chang T-H. Non-canonical expression of caudal during early embryogenesis in the pea aphid *Acyrtosiphon pisum*: maternal *cad*-driven posterior development is not conserved. *Insect Mol Biol.* 2013;22:442–55. <https://doi.org/10.1111/imb.12035>.
55. Ginzburg N, Cohen M, Chipman AD. Factors involved in early polarization of the anterior–posterior axis in the milkweed bug *Oncopeltus fasciatus*. *Genesis.* 2017;55:e23027. <https://doi.org/10.1002/dvg.23027>.
56. Novikova AV, Auman T, Cohen M, Oleynik O, Stahi-Hitin R, Gil E, Weisbrod A, Chipman AD. The multiple roles of *caudal* in early development of the milkweed bug *Oncopeltus fasciatus*. *Dev Biol.* 2020;467:66–76. <https://doi.org/10.1016/j.ydbio.2020.08.011>.
57. Nakamura T, Yoshizaki M, Ogawa S, Okamoto H, Shinmyo Y, Bando T, Ohuchi H, Noji S, Mito T. Imaging of transgenic cricket embryos reveals cell movements consistent with a syncytial patterning mechanism. *Curr Biol.* 2010;20:1641–7. <https://doi.org/10.1016/j.cub.2010.07.044>.
58. Donoughe S, Hoffmann J, Nakamura T, Rycroft CH, Extavour CG. Nuclear speed and cycle length co-vary with local density during syncytial blastoderm formation in a cricket. *Nat Commun.* 2022;13:3889. <https://doi.org/10.1038/s41467-022-31212-8>.
59. Taylor SE, Dearden PK. The *Nasonia* pair-rule gene regulatory network retains its function over 300 million years of evolution. *Development.* 2022;149:dev199632. <https://doi.org/10.1242/dev.199632>.
60. Choe CP, Miller SC, Brown SJ. A pair-rule gene circuit defines segments sequentially in the short-germ insect *Tribolium castaneum*. *Proc Natl Acad Sci.* 2006;103:6560–4. <https://doi.org/10.1073/pnas.0510440103>.
61. Wolff C, Sommer R, Schröder R, Glaser G, Tautz D. Conserved and divergent expression aspects of the *Drosophila* segmentation gene *hunchback* in the short germ band embryo of the flour beetle *Tribolium*. *Development.* 1995;121:4227–36. <https://doi.org/10.1242/dev.121.12.4227>.
62. Auman T, Chipman AD. Growth zone segmentation in the milkweed bug *Oncopeltus fasciatus* sheds light on the evolution of insect segmentation. *BMC Evol Biol.* 2018;18:178. <https://doi.org/10.1186/s12862-018-1293-z>.
63. Chipman AD, Arthur W, Akam M. Early development and segment formation in the centipede, *Strigamia maritima* (Geophilomorpha). *Evol Dev.* 2004;6:78–89. <https://doi.org/10.1111/j.1525-142X.2004.04016.x>.
64. Damen WGM, Weller M, Tautz D. Expression patterns of *hairly*, *even-skipped*, and *runt* in the spider *Cupiennius salei* imply that these genes were segmentation genes in a basal arthropod. *Proc Natl Acad Sci.* 2000;97:4515–9. <https://doi.org/10.1073/pnas.97.9.4515>.
65. Mittmann B, Wolff C. Embryonic development and staging of the cobweb spider *Parasteatoda tepidariorum* C. L. Koch, 1841 (syn.: *Achaearanea tepidariorum*; Araneomorpha; Theridiidae). *Dev Genes Evol.* 2012;222:189–216. <https://doi.org/10.1007/s00427-012-0401-0>.
66. Bruce HS, Jerz G, Kelly S, McCarthy J, Pomerantz A, Senevirathne G, Sherrard A, Sun DA, Wolff C, Patel NH. 2021. Hybridization Chain Reaction (HCR) in situ protocol. <https://doi.org/10.17504/protocols.io.bunznv6>
67. Pfaffl MW. A new mathematical model for relative quantification in real-time RT–PCR. *Nucleic Acids Res.* 2001;29: e45.
68. Schindelin J, Arganda-Carreras I, Frise E, Kaynig V, Longair M, Pietzsch T, Preibisch S, Rueden C, Saalfeld S, Schmid B, Tinevez J-Y, White DJ, Hartenstein V, Eliceiri K, Tomancak P, Cardona A. Fiji: an open-source platform for biological-image analysis. *Nat Methods.* 2012;9:676–82. <https://doi.org/10.1038/nmeth.2019>.

Publisher's Note

Springer Nature remains neutral with regard to jurisdictional claims in published maps and institutional affiliations.